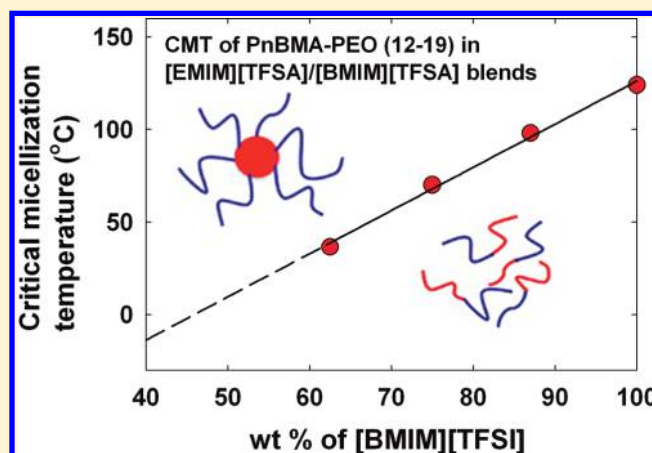


Poly(*n*-butyl methacrylate) in Ionic Liquids with Tunable Lower Critical Solution Temperatures (LCST)Hau-Nan Lee[†] and Timothy P. Lodge^{*,†,‡}[†]Department of Chemistry and [‡]Department of Chemical Engineering and Materials Science, University of Minnesota, Minneapolis, Minnesota 55455, United States

Supporting Information

ABSTRACT: We describe the lower critical solution temperature (LCST)-type phase behavior of poly(*n*-butyl methacrylate) (PnBMA) ($M = 13\,000$ and $48\,000$) dissolved in 1-alkyl-3-methylimidazolium bis{(trifluoromethyl) sulfonyl}amide ionic liquids (ILs). The temperature–composition phase diagrams of these PnBMA/IL systems are strongly asymmetric with the critical composition shifted to low concentrations of PnBMA. As the molecular weight increases from $13\,000$ to $48\,000$, the critical temperature decreases by $20\text{ }^{\circ}\text{C}$, and the critical composition shifts to a lower concentration. On the basis of the LCST of PnBMA, we designed a thermosensitive poly(*n*-butyl methacrylate)–poly(ethylene oxide) (PnBMA–PEO) diblock copolymer that exhibits a free chain/micelle transition in an IL as the temperature increases above the lower critical micellization temperature (LCMT). Furthermore, using IL blends as solvents, both the LCST of PnBMA and the LCMT of PnBMA–PEO can be tuned over a wide range by mixing two different alkyl methylimidazolium ILs without modifying the chemical structure of the polymers.



INTRODUCTION

Ionic liquids (ILs) are a class of solvents with appealing physical attributes such as negligible vapor pressure, good chemical and thermal stability, wide liquid temperature ranges, and high ionic conductivity. The desirable properties of ILs can be readily tuned for a given application by varying the chemical structures of the ions.¹ Composite polymer/IL systems are being considered for many applications, such as polymer electrolytes² in lithium batteries³ and solar cells.⁴ In addition, mixing ILs with suitable block polymers can solidify the ILs into particular spatial arrangements, such as membranes or gels,⁵ or to partition the ILs into coexisting phases, such as micelles.⁶ Possible applications include membranes for fuel cells and gas separations,⁷ gels for thin-film transistors,^{8,9} and micelles for molecular storage and transport systems.^{10,11} To optimize materials for these applications, understanding the phase behavior and the mutual miscibility of ILs and polymers over a wide range of temperature is essential.^{12,13}

The miscibility of a polymer and a solvent often varies as temperature changes. In general, the solubility of a nonionic polymer in water decreases as temperature increases, and several polymers exhibit LCST-type phase separation in water.^{14,15} On the other hand, the solubility of a polymer in an organic solvent often increases as temperature increases, and an UCST-type phase separation is often observed.¹⁶ Interestingly, in polymer/IL solutions, both UCST and LCST phase behavior have been reported. For

example, Ueki and Watanabe demonstrated the UCST phase behavior of poly(*N*-isopropylacrylamide) (PNIPAm) in 1-ethyl-3-methylimidazolium bis{(trifluoromethyl) sulfonyl}amide ([EMIM][TFSI]),¹⁷ in contrast to the LCST phase behavior of PNIPAm in water.¹⁸ Later, Watanabe and co-workers^{19–23} showed that poly(benzyl methacrylate) and its derivatives exhibit LCST phase behavior in 1-alkyl-3-methylimidazolium bis{(trifluoromethyl) sulfonyl}amide [C_n MIM][TFSI] and the transition temperature can be modified by randomly copolymerizing benzyl methacrylate with an azobenzene-containing monomer.²⁴ Watanabe and co-workers also observed an LCST-type phase behavior in poly(ethyl glycidyl ether)/[EMIM][TFSI] solutions.²⁵ In a recent work, Rodriguez et al.²⁶ performed a compositional analysis on biphasic liquid mixtures of poly(ethylene oxide) (PEO) and 1-alkyl-3-methylimidazolium chloride ([C_n MIM][Cl]) to obtain temperature–composition diagrams. The liquid–liquid equilibrium data²⁶ suggests LCST behavior, although the cloud point is not observed due to the solidification of both PEO and IL at low temperatures. Most recently, we reported that PEO is soluble in [EMIM][TFSI] over a wide range of temperature but exhibits an LCST-type phase behavior in 1-alkyl-3-methylimidazolium

Received: November 5, 2010

Revised: January 13, 2011

Published: February 15, 2011

tetrafluoroborate ($[C_n\text{MIM}][\text{BF}_4]$).²⁷ We also observed unusual temperature–composition phase diagrams in these PEO/ $[C_n\text{MIM}][\text{BF}_4]$ systems in which the cloud point curves are strongly asymmetric, with the critical composition shifted to high concentrations of PEO. Overall, these polymer/IL systems with phase boundaries either upon heating or cooling can be used to design bifunctional solvents for a dissolution/extraction process²⁶ and thermosensitive block copolymer/IL composites^{28–31} with potential applications in sensors, thermoresponsive gels, and actuators.

Understanding the LCST phase behavior of polymer/water solutions has been a challenging task. The narrow liquid range and high vapor pressure of water limit the experimental temperature range. In addition, adjusting the LCST value of a water-soluble polymer often relies on modifying the molecular structure of the polymer^{32–36} that requires extensive trial-and-error. Here, we report a model LCST polymer solution system comprising poly(*n*-butyl methacrylate) (PnBMA) and $[C_n\text{MIM}][\text{TFSA}]$ ionic liquids. The nonvolatility and good thermostability of ILs allow us to investigate the phase behavior over a wide range of temperature. More importantly, the solvation property of an IL can be easily adjusted by modifying the chemical structure of the ions and by blending two different ILs, which in turn allow the fine-tuning of the LCST value.

We find that the cloud point (CP) of this system can be altered by changing the molecular weight and the concentration of the PnBMA. As the molecular weight of PnBMA increases from 13 000 to 48 000, the critical temperature (T_c) decreases by 20 °C and the critical composition (w_c) shifts to a lower concentration. Furthermore, by varying the mixing ratio of IL blends (using ethyl, butyl, and hexyl methylimidazolium cations), the CP can be tuned from room temperature up to 250 °C. On the basis of these observations, a thermosensitive poly(*n*-butyl methacrylate)-poly(ethylene oxide) (PnBMA–PEO) diblock copolymer was designed. Dynamic light scattering (DLS) measurements show that the diblock copolymer exhibits a free chain/micelle transition as the temperature increases above the lower critical micellization temperature (LCMT). The LCMT of PnBMA–PEO can also be tuned over a wide range by varying the mixing ratio of IL blends. As expected, the LCMTs are close to the CPs of the corresponding PnBMA homopolymers.

■ EXPERIMENTAL SECTION

Materials. 1-Ethyl-3-methylimidazolium bis{(trifluoromethyl) sulfonyl} amide [EMIM][TFSA], 1-butyl-3-methylimidazolium bis{(trifluoromethyl) sulfonyl} amide [BMIM][TFSA], and 1-hexyl-3-methylimidazolium bis{(trifluoromethyl) sulfonyl} amide [HMIM][TFSA] were synthesized via the procedures described previously.^{37–39} ILs were used after drying in a vacuum oven at 50 °C for at least two days.

The materials used to synthesize PnBMA homopolymers and the PnBMA–PEO diblock copolymer are as follows. *n*-Butyl methacrylate (BMA) obtained from Sigma-Aldrich was purified by passing through a column filled with basic alumina to remove the inhibitor. PEO methylether ($M_n = 19\,000$, $M_w/M_n = 1.08$) was purchased from Polymer Source and purified by precipitation in *n*-hexane. 2-Bromo-2-methylpropanoyl bromide, triethylamine, ethyl 2-bromoisobutyrate (EBIB), N,N,N',N',N'' -pentamethyldiethylenetriamine (PMDETA), CuBr and all the other solvents were obtained from Sigma-Aldrich and used as received.

Atom Transfer Radical Polymerization (ATRP) of PnBMA Homopolymers and PnBMA–PEO Copolymer. PnBMA-13 and PnBMA-48 (the numbers indicate the molecular weight in kg/mol) were prepared by atom transfer radical polymerization (ATRP) using a procedure modified from the literature.⁴⁰ In brief, a dry Schlenk flask was filled with EBIB (0.09 g), PMDETA (0.08 g), and BMA (16 g). After a freeze–pump–thaw cycle, CuBr (0.066 g) was added into the mixture followed by another three freeze–pump–thaw cycles. The reaction was then carried out at 100 °C for 75 and 210 min to obtain PnBMA-13 and PnBMA-48, respectively, and then terminated by cooling the flask in an ice–water bath and opening it to the atmosphere. After evaporating the residual monomers under vacuum, the mixture was diluted with THF and then passed through an alumina column to remove the copper complex. Finally, the PnBMA was precipitated in cold methanol placed in a dry ice/isopropanol bath and then dried in a vacuum oven for four days. The polydispersities of PnBMA-13 and PnBMA-48 are 1.28 and 1.38, respectively. Both molecular weight and polydispersity were determined by size exclusion chromatography (SEC) performed on a Waters 150C ALC/GPC equipped with a refractive index detector and a multiangle light-scattering detector (Wyatt Technology).

The PnBMA–PEO block copolymer was synthesized by growing a PnBMA block from a PEO block via ATRP. A PEO–Br macroinitiator was first prepared by esterification of PEO methylether (PEO–OH) with 2-bromo-2-methylpropanoyl bromide in the presence of triethylamine in methylene chloride. PEO–Br macroinitiator (0.30 g) was then placed into a dry Schlenk flask together with *n*-butyl methacrylate (0.90 g), PMDETA (5 μL), and anisole (5 mL). After one freeze–pump–thaw cycle, CuBr (2 mg) was added into the solution under the protection of Ar. The mixture was then deoxygenated by three freeze–pump–thaw cycles. The flask was immersed in an oil bath at 75 °C for 20 h, and then the reaction was terminated by cooling the flask to 0 °C (ice–water bath) and opening it to the atmosphere. After evaporating the anisole and most of the residual monomers, the mixture was diluted with dichloromethane and passed through an alumina column to remove the copper complex. Finally, the block copolymer was obtained after drying it under vacuum for four days. The polymer has a 19 000 PEO block and a 12 000 PnBMA block as determined by ¹H NMR spectroscopy, and a polydispersity of $M_w/M_n = 1.20$ as determined by SEC (Supporting Information Figure S1).

Preparation of Polymer/ILs Solutions. Because of the high viscosities of ILs, it can be very difficult to directly dissolve a polymer. Direct mixing of PnBMA in [BMIM][TFSA] with vigorous stirring for more than three days still cannot achieve complete dissolution. Therefore, since the ionic liquids have essentially no vapor pressure, we utilized a cosolvent method to prepare polymer/ILs solutions. A strict procedure was applied to prepare polymer/IL solutions for CP and DLS measurements to minimize water and cosolvent content. PnBMA and ILs were first dissolved in ampules with the assistance of dichloromethane. The dichloromethane was then slowly evaporated under the purge of nitrogen followed by drying under vacuum (<50 mTorr) for at least 40 h to remove the residual cosolvent. Finally, the ampules were flame-sealed in an argon atmosphere to prevent moisture and degradation of components at high temperatures. The similar cosolvent method was applied to prepare PnBMA–PEO/IL solutions for the DLS measurements. After the removal of the cosolvent, the solutions were passed through 0.45 μm syringe filters into DLS glass tubes with an inner

diameter of 0.2 in. The tubes were then flame-sealed under vacuum to prevent moisture and degradation.

Cloud Point Measurements. The CPs of PnBMA/IL were determined by optical transmittance measurements at 632.8 nm at a heating rate of roughly 1 °C/min. The polymer solution was placed in a temperature-controlled oil bath. The temperature dependence of transmittance was monitored using a laser power detector (SPEX) while the solution was stirred. We define the CP values as the temperatures at which the transmittance drops to 80%.

Dynamic Light Scattering Measurements. The thermosensitive micellization behavior of PnBMA–PEO in [EMIM]–[TFSA]/[BMIM][TFSA] blends was investigated using dynamic light scattering (DLS). The details of the DLS measurements and data analysis can be found in previous publications.^{28,37} In brief, the DLS measurement was performed using a home-built experimental system includes a laser operating at 488 nm, a photomultiplier mounted onto a goniometer, and a Brookhaven correlator. In a typical DLS measurement, the intensity correlation functions, $g_2(q, t)$, at different temperatures were measured at a fixed 90° scattering angle with accumulation time ranged from 600 to 1200 s. The Siegert relation,⁴¹ $g_2(q, t) - 1 = g_1^2(q, t)$, was applied to transform the measured $g_2(q, t)$ to the electric field autocorrelation functions, $g_1(q, t)$. The $g_1(q, t)$ functions were then analyzed using the method of cumulants⁴² to obtain the average decay rate, Γ , which in turn was used to calculate the mutual diffusion coefficients, D_m . In the low concentration limit, D_m can be approximated by the tracer diffusion coefficient, D_t , and the mean hydrodynamic radii ($\langle R_h \rangle$) of micelles can be extracted through the Stokes–Einstein equation. An inverse Laplace transformation to the $g_1(q, t)$ function (REPES)⁴³ was employed to calculate the distribution of hydrodynamic radius. When the size distribution displayed a bimodal distribution, we fit the $g_1(q, t)$ function to a double exponential function to obtain the average decay rates from the two distinct distributions. The estimated uncertainty of the $\langle R_h \rangle$ obtained from a single angle (90°) dynamic light scattering measurement is ~ 5 –10%.

RESULTS AND DISCUSSION

LCST Phase Behavior of PnBMA in [BMIM][TFSA]. LCST phase behavior of PnBMA in ILs was investigated using cloud point (CP) measurements. The CP measurement is the simplest technique that can provide reliable indication of liquid–liquid phase separation in a polymer solution. In general the experimental CP lies between the coexistence curve (binodal) and stability limit (spinodal), but for polymer solutions is closer to the former. Figure 1a shows the temperature dependence of the transmittance at 632.8 nm for PnBMA-48 in [BMIM][TFSA] with different concentrations. The transmittance of 100% indicates a single-phase solution and a decrease in transmittance indicates that the solution undergoes liquid–liquid phase separation. At low temperatures, PnBMA-48 and [BMIM][TFSA] are completely miscible; a clear solution is observed. As the temperature increases above the LCST, the solution becomes cloudy and the transmittance quickly decreases. The CPs of 0.25, 0.5, 1, 2, and 4 wt % of PnBMA-48 in [BMIM][TFSA] are determined as 119, 113.5, 111, 108, and 107 °C, respectively. Similar LCST-type phase behavior was also observed for PnBMA-13 in [BMIM][TFSA] as shown in Figure 1b. The CPs of 0.25, 0.5, 1, 2, and 5 wt % of PnBMA-13 in [BMIM][TFSA] are identified as

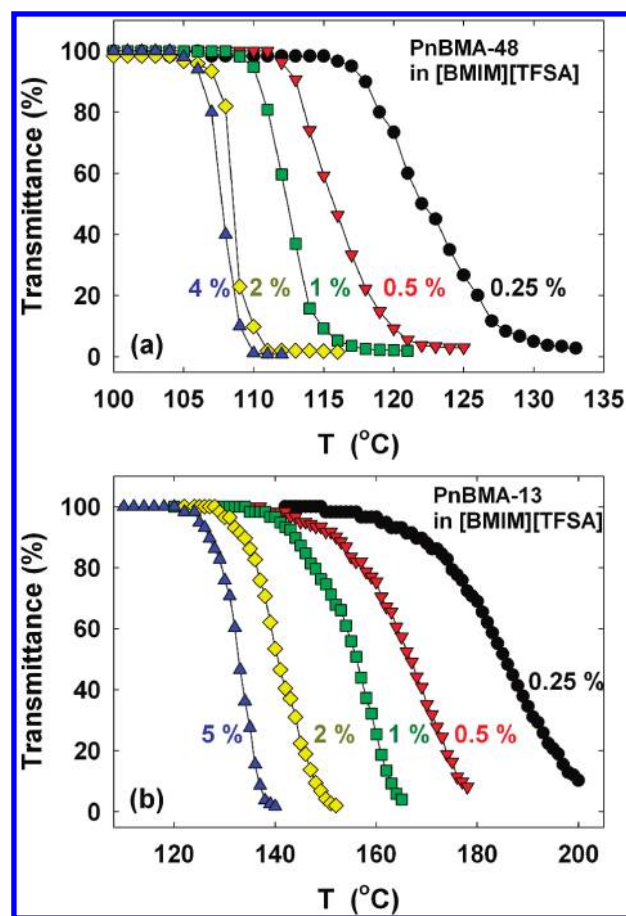


Figure 1. Temperature dependence of transmittance at 632.8 nm for (a) PnBMA-48 and (b) PnBMA-13 in [BMIM][TFSA] measured at a heating rate of ~ 1 °C/min. Weight fractions of PnBMA are indicated.

174.5, 157.5, 147.5, 136.5, and 129.5 °C, respectively. In both PnBMA/IL systems, the phase transition becomes broader as the concentration moves away from the critical composition (see Figure 2). The change in solubility with temperature in both systems is completely reversible.

Figure 2 shows the temperature–composition phase diagrams for PnBMA-48 and PnBMA-13 in [BMIM][TFSA]. The phase diagrams were constructed by plotting the CPs determined by the transmittance measurements illustrated in Figure 1. Both curves are convex downward, and the critical temperatures (T_c) are estimated to be ~ 107 and 127 °C with critical compositions (w_c) of roughly 5 and 10 wt % for PnBMA-48 and PnBMA-13, respectively. T_c decreases by 20 °C and w_c shifts to lower concentration as the molecular weight increases from 13 000 to 48 000. Such a trend is commonly observed in other polymer solutions and blends that exhibit LCST-type phase behavior.^{25,44}

From a thermodynamic point of view, a negative enthalpy of mixing (ΔH_{mix}) and a negative entropy of mixing (ΔS_{mix}) are essential for LCST phase behavior; this reflects the balance (or competition) between interactions such as Coulombic attractions, hydrogen bonding, and solvation effects among the polymer segments and the solvent molecules. Pioneering work by Watanabe and co-workers^{19–23} showed that poly(benzyl methacrylate) exhibits LCST phase behavior in $[C_n\text{MIM}][\text{TFSA}]$. They argued that in order for the LCST phase separation to occur the coexistence of structure-forming solvophobic groups and

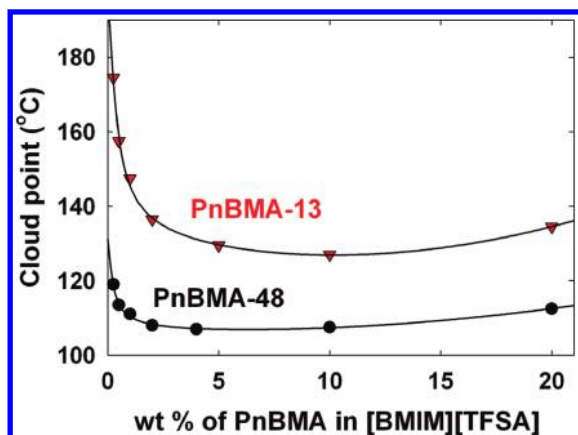


Figure 2. Temperature–composition phase diagrams for PnBMA-13 and PnBMA-48 in [BMIM][TFSA]. The CP values were determined from the transmittance measurements shown in Figure 1.

solvatophilic groups in the polymer is necessary. They also hypothesized that the negative ΔS_{mix} arises from the formation of ordered structures via cation- π interactions⁴⁵ between the IL cations and the aromatic groups in the polymer. Similarly, in the PnBMA/IL system, the coexistence of solvatophilic methacrylate groups and solvophobic *n*-butyl side chains likely plays an important role for the LCST phase behavior. We speculate that introducing the solvophobic *n*-butyl groups in IL results in oriented solvation around the *n*-butyl groups (analogous to the hydrophobic effect in aqueous polymer solutions),¹⁸ thereby providing the negative ΔS_{mix} . Consequently, specific orientations of the solvent molecules that arise upon polymer dissolution generate unfavorable entropic contributions to the free energy of mixing (ΔG_{mix}) as the temperature is increased, leading to phase separation. It is also possible that similar to PEO/IL²⁷ and organic solvent/IL solutions,⁴⁶ the oriented solvation by van der Waals interaction or hydrogen bonding act as driving force for the LCST phase behavior in our system, although we speculate that H-bonds play a minor role in this phenomenon. Clearly it will be of interest to explore the nature of the PnBMA/IL LCST system in more detail to quantify whether and how solvation effects are the driving force of the negative ΔS_{mix} .

PnBMA/IL Solutions with Tunable CP. To investigate how IL structure affects the phase behavior of PnBMA, we also studied the solubility of PnBMA in [EMIM][TFSA] and [HMIM][TFSA]. We found that PnBMA-48 is soluble in [HMIM][TFSA] from room temperature up to at least 250 °C. On the other hand, PnBMA-48 and [EMIM][TFSA] are not miscible even after cooling to 0 °C. No phase boundary can be identified in either IL. To tune the values of CP, we then used IL blends as solvents. Figure 3a shows the transmittance measurements of 2 wt % of PnBMA-48 in [EMIM][TFSA]/[BMIM][TFSA] blends with different mixing ratios. Not surprisingly, in all IL blends, PnBMA-48 shows reversible LCST phase behavior, and the CP value decreases as the weight fraction of [BMIM][TFSA] decreases. Similar results are also observed for 2 wt % PnBMA-13 in [EMIM][TFSA]/[BMIM][TFSA] blends (data not shown). In Figure 3b, we plot the CPs of PnBMA-48 and PnBMA-13 in IL blends as a function of the weight fraction of [BMIM][TFSA]. The CPs decrease almost linearly from 108 °C for PnBMA-48 and 136.5 °C for PnBMA-13 to room temperature as the weight fraction of [BMIM][TFSA] decreases. Likewise, as shown in Figure 4, using [BMIM][TFSA]/[HMIM][TFSA] blends as solvents, the CP values of PnBMA-48 in ILs

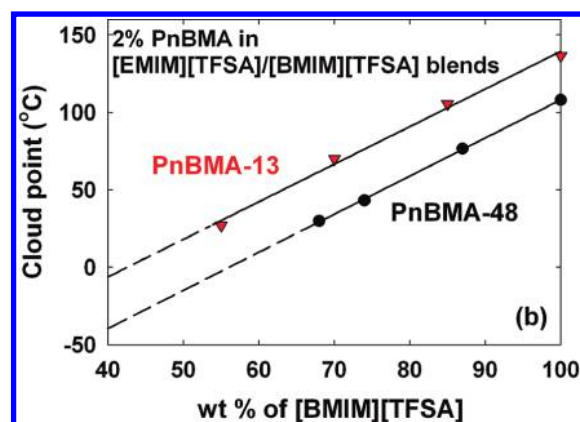
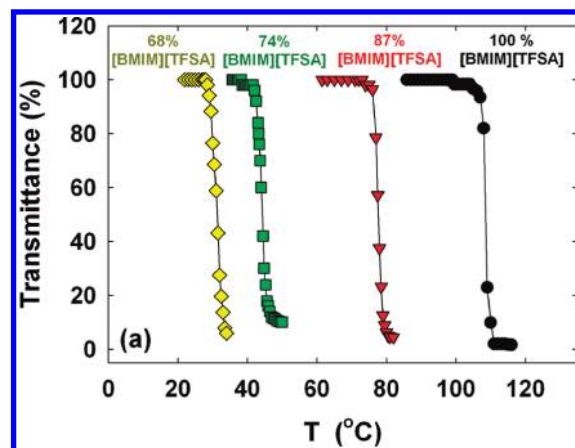


Figure 3. LCST phase behavior of PnBMAs in [EMIM][TFSA]/[BMIM][TFSA] blends. (a) Temperature dependence of transmittance at 632.8 nm for 2 wt % PnBMA-48. Weight fraction of [BMIM][TFSA] in the IL blends are indicated. (b) The CPs of PnBMA-48 and PnBMA-13 as a function of the weight fraction of [BMIM][TFSA] in the IL blends. The lines are linear fits to the data.

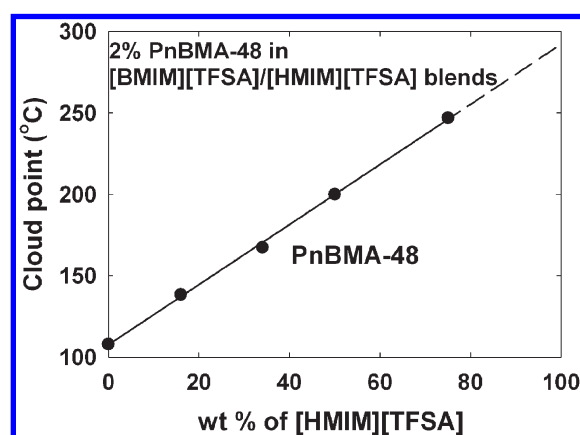


Figure 4. The CPs of PnBMA-48 as a function of the weight fraction of [HMIM][TFSA] in [BMIM][TFSA]/[HMIM][TFSA] blends. The line is a linear fit to the data.

increase almost linearly from 108 up to 247 °C (close to the limit of the CP measurement instrument) as the weight fraction of [HMIM][TFSA] increases. The results in Figures 3b and 4 therefore indicate that the value of CP can be easily controlled

over a wide range by appropriately adjusting the mixing ratio of two ILs.

Figures 3 and 4 indicate that the length of the side chain in the imidazolium ring has a significant impact on the solubility of PnBMA in ILs; a small increase in alkyl side chain length ($C_2 \rightarrow C_4 \rightarrow C_6$) results in huge increase in the CP. This result is consistent with the increase in CP with alkyl chain length in PEO/ $[C_n\text{MIM}][\text{BF}_4]$ ²⁷ and poly(benzyl methacrylate)/ $[C_n\text{MIM}][\text{TFSA}]$.¹⁹ Watanabe and co-workers argued that this observation may be due to the extended microphase segregation induced by the longer alkyl chain length on the imidazolium cation.¹⁹ Several recent simulations^{47–49} suggest that imidazolium-based ILs form segregated structures with polar ionic domains and non-polar alkyl chain domains. Increasing the alkyl chain length may increase the extent of microphase segregation, which in turn lowers the entropy of the ILs. As a result, the loss of mixing entropy induced by the formation of ordered structure between PnBMA and ILs would be reduced, leading to an increase in the LCST. It is also likely that the extended nonpolar alkyl domains enhance the interactions between the IL and the alkyl main chain and/or butyl side chains of the polymer, which consequently lowers the mixing enthalpy and causes an increase in the LCST.

The linear trend of change in transition temperature in PnBMA/ILs systems is also observed in other polymer/ILs systems that exhibit either LCST such as poly(benzyl methacrylate)¹⁹ and PEO,^{27,28} or UCST such as PNIPAm.²⁸ It is likely that this linear trend can be generally observed in any polymer/IL blends with a critical phase behavior, where the two ILs are structurally very similar. In contrast, this linearity is not typical in polymer/molecular solvent systems such as PNIPAm^{50,51} and poly(methyl methacrylate)⁵² in water/organic solvent mixtures, or ionic liquids in water/ethanol mixtures.⁵³ For example, Schild, Muthukumar, and Tirrell⁵¹ showed that there is an initial decrease in the CP of PNIPAm and then a sudden increase as the fraction of organic solvent (methanol, THF, or dioxane) in water increases. They also showed that the CP of poly(vinyl methyl ether) in water/methanol mixtures increase as the fraction of methanol increases, but the trend is not linear. It is likely that organic solvents modify the hydrogen bonding and the water structure substantially as the fraction of organic solvent increases. On the other hand, the linear trend of UCST or LCST in polymer/ILs suggests that mixing two different ILs does not change the nature of the interactions between polymer and ions very much. Therefore, it is close to an ideal random mixing process.

Thermosensitive Self-Assembly of PnBMA–PEO Diblock Copolymer in IL Blends. To further explore the phase behavior of PnBMA in ILs, we designed a thermosensitive PnBMA–PEO (12–19) diblock copolymer synthesized via ATRP. The PEO block is soluble in $[\text{EMIM}][\text{TFSA}]$ and $[\text{BMIM}][\text{TFSA}]$ from room temperature up to at least 200 °C, while PnBMA block shows an LCST in $[\text{EMIM}][\text{TFSA}]/[\text{BMIM}][\text{TFSA}]$ blends as shown in Figure 3. Therefore, a thermoresponsive free chain to micelle transition is anticipated. Figure 5a shows the scattering intensity at 90° from DLS measurements as a function of temperature for 1 wt % PnBMA–PEO in $[\text{EMIM}][\text{TFSA}]/[\text{BMIM}][\text{TFSA}]$ blends with different mixing ratios. Low levels of scattering intensity indicate molecular dissolution and increased scattering intensity indicates the formation of micelles. The results suggest that, in all four IL blends, PnBMA–PEO dissolves at low temperatures and self-assembles into micelles as the temperature increase above the lower critical micellization temperature (LCMT).

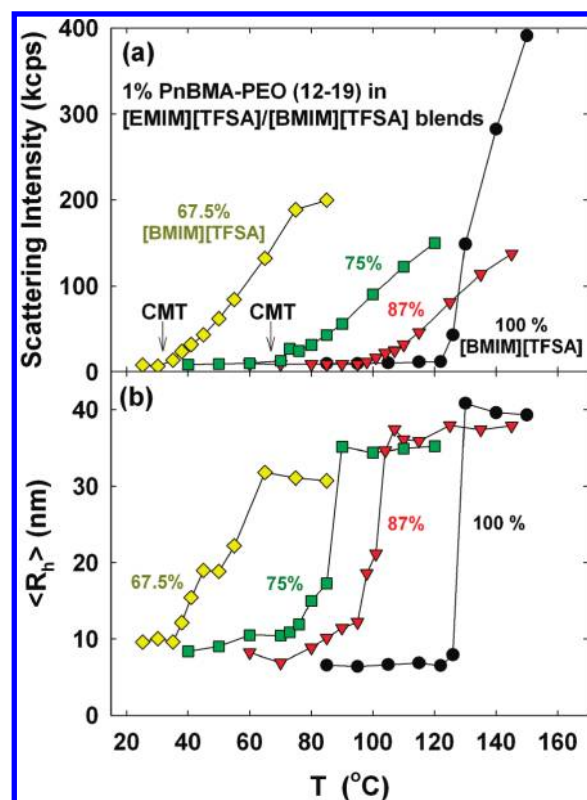


Figure 5. Micellization of PnBMA–PEO (12–19) in $[\text{EMIM}][\text{TFSA}]/[\text{BMIM}][\text{TFSA}]$ blends. Temperature dependence of (a) scattering intensity and (b) hydrodynamic radius for 1 wt % of PnBMA–PEO in IL blends. Weight fraction of $[\text{BMIM}][\text{TFSA}]$ in the IL blends are indicated.

Figure 5b displays the corresponding mean hydrodynamic radius ($\langle R_h \rangle$) as a function of temperature for 1 wt % PnBMA–PEO in ILs obtained from cumulant or double exponential fits. At temperatures lower than the LCMT, the $\langle R_h \rangle$ shown in Figure 5b is obtained from a double exponential fit; only the smaller values are plotted, since large aggregates in this temperature range represent a very small fraction. As shown in Figure 6a, b, at low temperatures the size distribution for PnBMA–PEO in $[\text{BMIM}][\text{TFSA}]$ displays a bimodal distribution. The small R_h peak corresponds to single polymer chains, whereas the large R_h peak indicates the existence of large aggregates. These aggregates may arise from a trace amount of PnBMA homopolymers that result in “anomalous micellization”⁵⁴ and cause the aggregation, even though such homopolymers are not apparent in the SEC trace. At higher temperatures, the PnBMA homopolymers are incorporated into the core of the PnBMA–PEO micelles, so that only one peak is seen in the distribution. Given that the overall scattering intensity in this temperature range is very low (Figure 5a) and the scattering intensity is roughly proportional to R_h^6 (Rayleigh approximation), the number fraction of single polymer chains at these temperatures is estimated to be more than 99.99%.

At temperatures above the LCMT, the $\langle R_h \rangle$ is determined from cumulant analysis, since a monomodal distribution was obtained (Figure 6c–e), indicating the formation of well-defined micelles. For all four copolymer/ILs systems, both scattering intensity (Figure 5a) and $\langle R_h \rangle$ (Figure 5b) results indicate that there is an LCMT-type phase transition temperature. Therefore, we conclude that the block copolymers dissolve at low temperatures and form PnBMA-core and PEO-corona micelles above the LCMT.

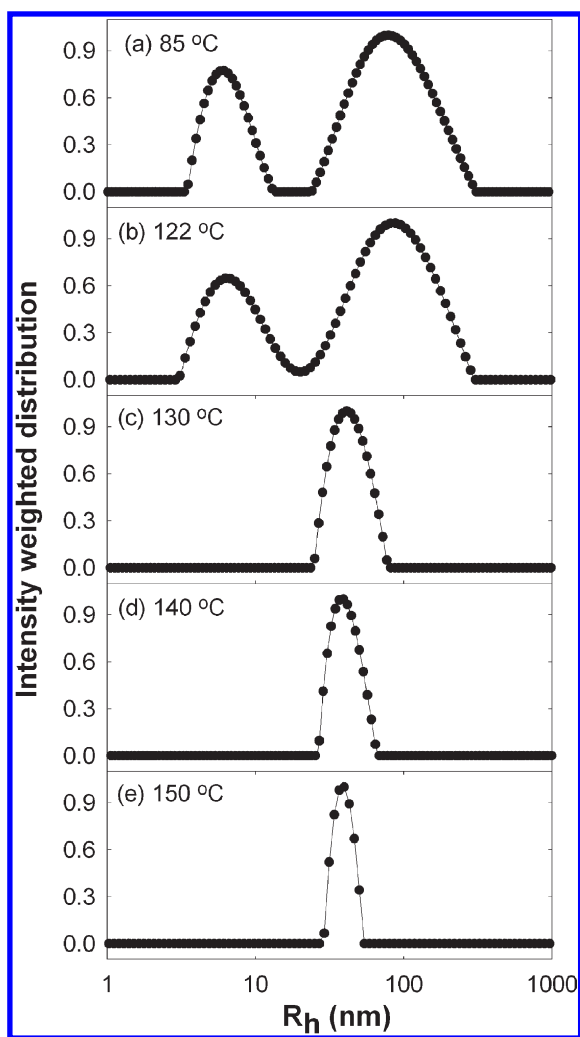


Figure 6. Intensity weighted distribution of hydrodynamic radius for 1 wt % PnBMA-PEO in [BMIM][TFSA] at different temperatures.

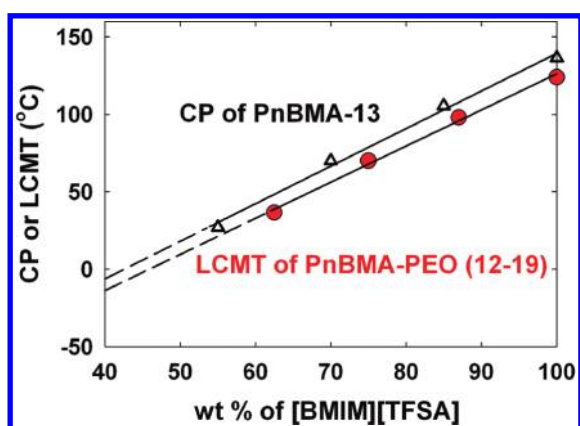


Figure 7. The LCMTs determined from the DLS measurements (Figure 5) as a function of the weight fraction of [BMIM][TFSA] in IL blends. The CPs of PnBMA-13 (Figure 3) are also plotted. The lines are linear fits to the data. Similar linear trends are observed in CP and LCMT data.

Figure 7 illustrates the LCMT values determined from DLS measurements shown in Figure 5. For a comparison, the CPs of PnBMA-13 obtained from transmittance measurements are also

plotted in the same figure. As expected, similar to the trend of linearity for CPs of PnBMA, the LCMT values decrease almost linearly as the weight fraction of [BMIM][TFSA] decreases. This result indicates that not only the CP values, but also the LCMT values can be easily controlled by appropriately adjusting the mixing ratio of two ILs, without modifying the chemical structure of the polymer.

CONCLUSION

In this paper, we report a new class of polymer that exhibits LCST-type phase behavior in ILs. Temperature–composition phase diagrams for two molecular weight of PnBMA in [BMIM]-[TFSA] are strongly asymmetric with the critical composition (w_c) shifted to low concentrations of PnBMA. An increase in molecular weight from 13 000 to 48 000 results in a reduction of critical temperature (T_c) by 20 °C. The length of the alkyl chain in the imidazolium cation has a significant influence on the miscibility of this polymer/IL system. Using IL blends as solvents, the CP of PnBMA can be easily tuned over a wide range by adjusting the mixing ratio of two ILs. In addition, a PnBMA-PEO/[BMIM]-[TFSA] solution that exhibits thermosensitive free chain/micelle self-assembly was designed. As expected, the free chain to micelle transition temperatures are near the CPs of PnBMA/IL. Future work will be focused on understanding the contribution of solvation effects to the negative entropy of mixing. The influence of the polymer side chain length on the LCST behavior will be explored. The discovery of the LCST phase behavior of PnBMA in ILs with a wide usable temperature range is expected to have potential applications on the design of new thermosensitive materials or solutions for dissolution/separation processes.

ASSOCIATED CONTENT

S Supporting Information. SEC trace of PnBMA-PEO block copolymer. This material is available free of charge via the Internet at <http://pubs.acs.org>.

AUTHOR INFORMATION

Corresponding Author

*E-mail: lodge@umn.edu.

ACKNOWLEDGMENT

This work was supported by the National Science Foundation through Award DMR-0804197. Helpful discussions with Dr. Takeshi Ueki and Professor M. Watanabe are appreciated.

REFERENCES

- (1) Hough, W. L.; Smiglak, M.; Rodriguez, H.; Swatoski, R. P.; Spear, S. K.; Daly, D. T.; Pernak, J.; Grisel, J. E.; Carliss, R. D.; Soutullo, M. D.; Davis, J. H.; Rogers, R. D. *New J. Chem.* **2007**, *31*, 1429–1436.
- (2) Susan, M. A.; Kaneko, T.; Noda, A.; Watanabe, M. *J. Am. Chem. Soc.* **2005**, *127*, 4976–4983.
- (3) Shin, J. H.; Henderson, W. A.; Passerini, S. *J. Electrochem. Soc.* **2005**, *152*, A978–A983.
- (4) Wang, M.; Xiao, X. R.; Zhou, X. W.; Li, X. P.; Lin, Y. *Sol. Energy Mater. Sol. Cells* **2007**, *91*, 785–790.
- (5) He, Y. Y.; Boswell, P. G.; Buhlmann, P.; Lodge, T. P. *J. Phys. Chem. B* **2007**, *111*, 4645–4652.
- (6) He, Y. Y.; Li, Z. B.; Simone, P.; Lodge, T. P. *J. Am. Chem. Soc.* **2006**, *128*, 2745–2750.
- (7) Bara, J. E.; Lessmann, S.; Gabriel, C. J.; Hatakeyama, E. S.; Noble, R. D.; Gin, D. L. *Ind. Eng. Chem. Res.* **2007**, *46*, 5397–5404.

- (8) Cho, J. H.; Lee, J.; He, Y.; Kim, B.; Lodge, T. P.; Frisbie, C. D. *Adv. Mater.* **2008**, *20*, 686.
- (9) Cho, J. H.; Lee, J.; Xia, Y.; Kim, B.; He, Y. Y.; Renn, M. J.; Lodge, T. P.; Frisbie, C. D. *Nat. Mater.* **2008**, *7*, 900–906.
- (10) He, Y. Y.; Lodge, T. P. *J. Am. Chem. Soc.* **2006**, *128*, 12666–12667.
- (11) Bai, Z. F.; He, Y. Y.; Young, N. P.; Lodge, T. P. *Macromolecules* **2008**, *41*, 6615–6617.
- (12) Rodriguez, H.; Rogers, R. D. *Fluid Phase Equilib.* **2010**, *294*, 7–14.
- (13) Winterton, N. J. *Mater. Chem.* **2006**, *16*, 4281–4293.
- (14) Crespy, D.; Rossi, R. N. *Polym. Int.* **2007**, *56*, 1461–1468.
- (15) Galaev, I. Y.; Mattiasson, B. *Enzyme Microb. Technol.* **1993**, *15*, 354–366.
- (16) Bae, Y. C.; Shim, J. J.; Soane, D. S.; Prausnitz, J. M. *J. Appl. Polym. Sci.* **1993**, *47*, 1193–1206.
- (17) Ueki, T.; Watanabe, M. *Chem. Lett.* **2006**, *35*, 964–965.
- (18) Schild, H. G. *Prog. Polym. Sci.* **1992**, *17*, 163–249.
- (19) Kodama, K.; Nanashima, H.; Ueki, T.; Kokubo, H.; Watanabe, M. *Langmuir* **2009**, *25*, 3820–3824.
- (20) Ueki, T.; Arai, A. A.; Kodama, K.; Kaino, S.; Takada, N.; Morita, T.; Nishikawa, K.; Watanabe, M. *Pure Appl. Chem.* **2009**, *81*, 1829–1841.
- (21) Ueki, T.; Karino, T.; Kobayashi, Y.; Shibayama, M.; Watanabe, M. *J. Phys. Chem. B* **2007**, *111*, 4750–4754.
- (22) Ueki, T.; Watanabe, M. *Langmuir* **2007**, *23*, 988–990.
- (23) Ueki, T.; Watanabe, M. *Macromolecules* **2008**, *41*, 3739–3749.
- (24) Ueki, T.; Yamaguchi, A.; Ito, N.; Kodama, K.; Sakamoto, J.; Ueno, K.; Kokubo, H.; Watanabe, M. *Langmuir* **2009**, *25*, 8845–8848.
- (25) Tsuda, R.; Kodama, K.; Ueki, T.; Kokubo, H.; Imabayashi, S.; Watanabe, M. *Chem. Commun.* **2008**, 4939–4941.
- (26) Rodriguez, H.; Francisco, M.; Rahman, M.; Sun, N.; Rogers, R. D. *Phys. Chem. Chem. Phys.* **2009**, *11*, 10916–10922.
- (27) Lee, H. N.; Lodge, T. P. *J. Phys. Chem. Lett.* **2010**, *1*, 1962–1966.
- (28) Lee, H. N.; Bai, Z. F.; Newell, N.; Lodge, T. P. *Macromolecules* **2010**, *43*, 9522–9528.
- (29) Tamura, S.; Ueki, T.; Ueno, K.; Kodama, K.; Watanabe, M. *Macromolecules* **2009**, *42*, 6239–6244.
- (30) Ueki, T.; Watanabe, M.; Lodge, T. P. *Macromolecules* **2009**, *42*, 1315–1320.
- (31) He, Y. Y.; Lodge, T. P. *Macromolecules* **2008**, *41*, 167–174.
- (32) Takei, Y. G.; Aoki, T.; Sanui, K.; Ogata, N.; Okano, T.; Sakurai, Y. *Bioconjugate Chem.* **1993**, *4*, 341–346.
- (33) Rackaitis, M.; Strawhecker, K.; Manias, K. *J. Polym. Sci., Part B: Polym. Phys.* **2002**, *40*, 2339–2342.
- (34) Virtanen, J.; Baron, C.; Tenhu, H. *Macromolecules* **2000**, *33*, 336–341.
- (35) Bokias, G.; Hourdet, D.; Iliopoulos, I. *Macromolecules* **2000**, *33*, 2929–2935.
- (36) Laschewsky, A.; Reka, E. D.; Wischerhoff, E. *Macromol. Chem. Phys.* **2001**, *202*, 276–286.
- (37) Meli, L.; Santiago, J. M.; Lodge, T. P. *Macromolecules* **2010**, *43*, 2018–2027.
- (38) Bai, Z. F.; Lodge, T. P. *J. Phys. Chem. B* **2009**, *113*, 14151–14157.
- (39) Bai, Z. F.; Lodge, T. P. *J. Am. Chem. Soc.* **2010**, *132*, 16265–16270.
- (40) Colombani, O.; Ruppel, M.; Schubert, F.; Zettl, H.; Pergushov, D. V.; Muller, A. H. E. *Macromolecules* **2007**, *40*, 4338–4350.
- (41) Brown, W. *Dynamic Light Scattering: The Method and Some Applications*; Oxford University Press: New York, 1993.
- (42) Koppel, D. E. *J. Chem. Phys.* **1972**, *57*, 4814–4820.
- (43) Jakes, J. *Collect. Czech. Chem. Commun.* **1995**, *60*, 1781–1797.
- (44) Jung, J. G.; Bae, Y. C. *J. Polym. Sci., Part B: Polym. Phys.* **2010**, *48*, 162–167.
- (45) Ma, J. C.; Dougherty, D. A. *Chem. Rev.* **1997**, *97*, 1303–1324.
- (46) Lachwa, J.; Szydłowski, J.; Najdanovic-Visak, V.; Rebelo, L. P. N.; Seddon, K. R.; da Ponte, M. N.; Esperanca, J.; Guedes, H. J. R. *J. Am. Chem. Soc.* **2005**, *127*, 6542–6543.
- (47) Wang, Y. T.; Voth, G. A. *J. Am. Chem. Soc.* **2005**, *127*, 12192–12193.
- (48) Lopes, J.; Padua, A. A. H. *J. Phys. Chem. B* **2006**, *110*, 3330–3335.
- (49) Lopes, J. N. C.; Gomes, M. F. C.; Padua, A. A. H. *J. Phys. Chem. B* **2006**, *110*, 16816–16818.
- (50) Winnik, F. M.; Ringsdorf, H.; Venzmer, J. *Macromolecules* **1990**, *23*, 2415–2416.
- (51) Schild, H. G.; Muthukumar, M.; Tirrell, D. A. *Macromolecules* **1991**, *24*, 948–952.
- (52) Cowie, J. M. G.; Mohsin, M. A.; McEwen, I. J. *Polymer* **1987**, *28*, 1569–1572.
- (53) Swatloski, R. P.; Visser, A. E.; Reichert, W. M.; Broker, G. A.; Farina, L. M.; Holbrey, J. D.; Rogers, R. D. *Green Chem.* **2002**, *4*, 81–87.
- (54) Lodge, T. P.; Bang, J.; Hanley, K. J.; Krocak, J.; Dahlquist, S.; Sujan, B.; Ott, J. *Langmuir* **2003**, *19*, 2103–2109.